RESEARCH PERFORMANCE PROGRESS REPORT

FEDERAL AGENCY:
U.S. DOE/NETL
NATIONAL ENERGY TECH LAB
3610 Collins Ferry Road
PO Box 880
Morgantown, WV 26507-0880

FEDERAL GRANT OR OTHER IDENTIFYING NUMBER BY AGENCY:

DE-FE0029059

PROJECT TITLE:
Remote Methane Sensor for Emissions from Pipelines and
Compressor Stations Using Chirped-Laser Dispersion Spectroscopy

PI NAME:
Mark Zondlo
Associate Professor of Civil and Environmental Engineering
Email: mzondlo@princeton.edu
Phone: (609) 258-5037
Fax: (609) 258-2760

CO-PI NAME:
Gerard Wysocki
Associate Professor of Electrical Engineering
Email: gwysocki@princeton.edu

SUBMISSION DATE:
September 7, 2018

DUNS NUMBER: 00-248-4665

RECIPIENT ORGANIZATON:
Princeton University
Princeton, NJ 08544

PROJECT/GRANT PERIOD
10/1/2016 - 3/31/2020

REPORTING PERIOD END DATE
June 30, 2018

REPORTING TERM OR FREQUENCY
Quarterly (for period 3/1/18 to 6/30/18)

Mark Zondlo, Submitting Official

1. **Cover Page (previous)**

2. Accomplishments

2a. Goals

Leak rates of methane (CH_4) from the natural gas supply chain result in lost profit from unsold product, public safety and property concerns due to potential explosion hazards, and a potentially large source of economic damages from legal liabilities. Yet large measurement challenges exist in identifying and quantifying CH_4 leak rates along the vast number and type of components in the natural gas supply chain. This is particularly true of the "midstream" components of gathering, processing, compression, transmission, and storage.

This project will develop and deploy new advances in chirped laser dispersion spectroscopy (CLaDS) to make an airborne-based sensor for remote detection of methane leaks from pipelines, compressor stations, and other midstream infrastructure. Leaks of methane not detected through routine pipeline patrols and only inferred by indirect methods (e.g. dead vegetation). The proposed heterodyne-enhanced chirped modulated CLaDS (HE-CM-CLaDS) system will offer ability to perform measurements with low light returns, immunity to back-scattered light intensity fluctuations and high linearity and extended dynamic range of concentration detection.

The proposed effort will use a range-resolved, integrated-path spectroscopic technique to remotely identify leaks along pipelines and other related facilities. The instrument will be capable of being deployed on a vehicle, manned aircraft, or making three-dimensional tomographic images with appropriate flight patterns of a microdrone or by passive sampling. Manned aircraft already patrol pipelines for threat detection and visible signs of leak on monthly timescales. Yet there exist no sensors that can show the necessary sensitivity to detect leaks from such a platform. In this project, we will develop, field test, validate, and demonstrate the system over a pipeline corridor. The system proposed here will target the following specifications:

- Open-path methane measurement
- Sensitivity to methane will be in the <1ppmv-m/Hz$^{1/2}$
- Simultaneous range measurement for 3D tomographic reconstruction
- Ability to perform sensitive CH_4 measurements by scattering from natural hard-targets

The technical innovation is using range-resoled, chirped modulation-chirped laser dispersion spectroscopic detection for methane quantification, which will provide the most robust yet relatively inexpensive hardware solution while delivering sensing performance needed for the target application. The proposed method utilizes optical phase of the detected light for molecular detection and thus is insensitive to fluctuations in intensity of backscattered light within four orders of magnitude, a key feature necessary when scanning through natural hard targets. The proposed system will be validated by controlled tracer releases when integrated onto vehicle and aircraft-based platforms.

Commercial translation to the marketplace will occur by partnering with a pipeline service provider, American Aerospace Technologies, Inc., for flight demonstrations to their clients in the gas, oil, and pipeline industries. In this way, feedback on the sensor performance and attributes will be efficient and minimize delays in bringing the technologies to the private sector. Benefits of a commercial sensor with these capabilities include reductions of leaks for pipeline operators (more profit), earlier detection of leaks to avoid catastrophic explosion hazards (employee safety, public health and mitigation of property damage), and reduced methane emissions to the atmosphere (improving air quality).

2b. Major activities, results, and outcomes/achievements

Task 1: Project Management, Planning, and Reporting
Status: Completed
Deliverables: Project Management Plan was March 20, 2017 and accepted by the Project Manager via email notification on March 27, 2017.
Milestone A: Data Management Plan submitted → milestone achieved on March 20, 2017.

Task 2: Development of HE-CM-CLaDS sensor
Milestone B: Develop the HE-CM-CLaDS sensor → milestone achieved on February 28, 2018; email and short report sent to program manager on March 22, 2018

Task 3: Laboratory testing of system parameters
Status: In-progress

Research progress made:

- **Noise modeling and experimental validation for HE-CLaDS and conventional CLaDS performance**
- **Updated characterization of the system**

Task 3.1: Noise modeling for HE-CLaDS and conventional CLaDS
We have analyzed the noise performance of HE-CLaDS in comparison with CLaDS to determine a quantitative condition for choosing between the two methods depending on the application setting (e.g. intensity of backscattered light back to the sensor).

The noise model for conventional CLaDS has already been published [1]. A similar approach is used for developing HE-CLaDS noise model was developed and confirmed as part of this project. In both conventional CLaDS and HE-CLaDS, the final signal and noise are measured in units of frequency (Hz) after frequency demodulation. The noise floor is shaped by the process of the time derivative of the phase demodulated signal. In HE-CLaDS, an additional step of beatnote mixing is inserted between amplitude acquisition and phase demodulation, which leads to some of the main differences in noise power spectrum from that of CLaDS [1].

In conventional CLaDS, due to self-coherence between beating optical fields, a sharp beatnote is formed in the RF domain at the PD with carrier power:

$$C = \frac{A^2}{2} = \frac{(\eta\sqrt{P_1 P_2}R)^2}{2} ,$$

where A is the beatnote current amplitude, η is heterodyne efficiency (and can be considered unity for conventional CLaDS due to spatial optical field coherence), $P_{1,2}$ is the optical power carried by the two probing fields, and R is responsivity of the detector. The white noise floor is either dominated by detector noise, or is shot noise limited for higher receiving optical power. In the case of conventional CLaDS, the noise power spectrum after frequency demodulation is inversely proportional to carrier power, with a quadratic term f^2 multiplied to the white noise shape as a result of time differentiation. The final noise power is integrated over the demodulation bandwidth, which is typically 11 times the modulation frequency of the laser to recover the signal [1]. The final noise power of conventional CLaDS is proportional to the following:

$$\frac{NB^3}{3A^2} = \frac{NB^3}{(\eta\sqrt{P_1P_2}R)^2}$$

If the two probing optical fields have the same optical power $P_1 = P_2 = P_{sig}$, then the final noise power is inversely proportional to $P_{sig}{}^2$, or the noise will decrease quadratically as the received optical power increases.

In HE-CLaDS, at the demodulation stage, the beatnotes formed by the optical local oscillator for enhancement and the probing fields are broadened as the self-coherence no longer holds due to time-delay and non-linear laser chirping. Without considering laser chirping effect, the beatnotes carry a Lorentzian lineshape with the total beatnote power

$$C_i = \frac{A_i{}^2}{2} = \frac{(\eta\sqrt{P_{LO}P_i}R)^2}{2}$$

spreading over the broadened bandwidth. Here the heterodyne efficiency can no longer be assumed to be 1 for diffusive target. The mixing process requires bandpass filtering which includes at least one full width at half maximum (FWHM) of the beatnote to cancel out phase noise and preserve information. After non-linear mixing, the two beatnotes will collapse into a sharp beatnote with new carrier power

$$C = \frac{(A_1A_2)^2}{2} = \frac{(\eta^2 P_{LO}\sqrt{P_1P_2}R^2)^2}{2}.$$

The mixing process also produces two types of noise floors: "Type I" from white noise and white noise mixing, and "Type II" from phase induced amplitude noise and white noise mixing. After phase and frequency demodulation, Type I noise is inversely proportional to the new C, and thus inversely proportional to $P_{sig}{}^2$ similar to CLaDS, but Type II noise is inversely proportional to only P_{sig}. For both types of noise, the presence of P_{LO} will significantly lower the demodulated noise power in the end. When received optical power P_{sig} is low, Type I noise dominates and decreases quadratically with increased P_{sig}, until Type II noise starts to dominate. Since Type II noise decreases more slowly with increased P_{sig} that the noise of conventional CLaDS does, eventually conventional CLaDS will surpass HE-CLaDS performance at higher received power. This was confirmed experimentally as shown in Figure 1 below.

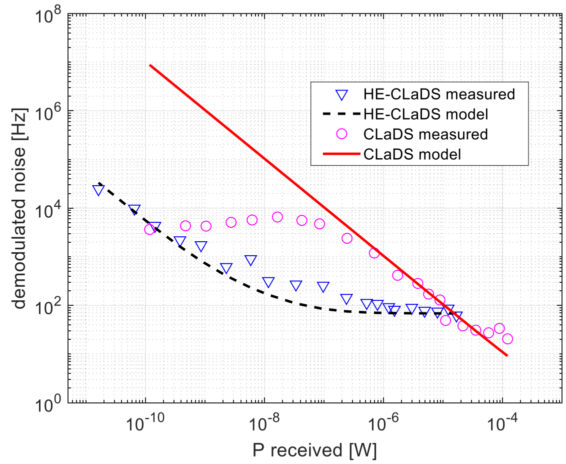

Figure 1. Noise models of HE-CLaDS and CLaDS as demodulated noise with respect to received optical power.

The lines are predicting models, and individual points are experimental data collected in lab. The received power is varied by using a variable attenuator, and is read through the detector DC output. Both the local oscillator enhancement and noise type switching can be seen clearly in the HE-CLaDS data.

The result of the noise analysis suggests that for the given system, when received optical power is below 10 μW, HE-CLaDS should be chosen for enhancement; whereas for above 10 μW signal, conventional CLaDS is a better choice.

[1] Genevieve Plant, Andreas Hangauer, and Gerard Wysocki. "Fundamental noise characteristics of chirped laser dispersion spectroscopy." IEEE Journal of Selected Topics in Quantum Electronics 23.2 (2017): 147-156.

Task 3.2: Updated characterization of the HE-CLaDS system

There are three proposed goals for the performance of the system: 1 ppm-m/√Hz for methane concentration measurement, <0.1 m/√Hz precision for ranging measurement, and > 10 dB enhancement on carrier to noise ratio using heterodyne enhancement.

For methane and ranging measurements, at least two sets of experiments have been conducted to characterize the system: one with fiber coupled system in lab (well-controlled environment) and one with free space transmitter/receiver in lab and/or hallway (temperature, pressure and concentration of methane not controlled). The free space set up also loses more optical power in the collecting optics than all fiber-coupled system. As noted previously from Task 3.1, lower received power leads to higher noise proportionally. Temperature and pressure drifts will cause signal drift if not well characterized. The results are summarized in Allan deviation plots in Figure 2. Allan plots quantify the noise and drift in a sensor at different integration times. White noise processes have a slope of -1/2 in these plots, and deviations from white noise at longer integration times indicate longer term drift in a measurement.

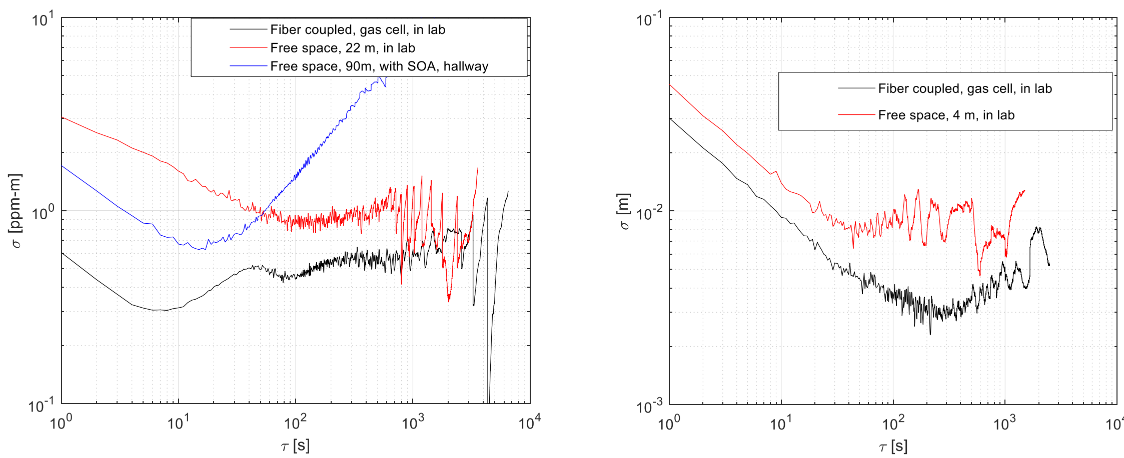

Figure 2. (a) Methane concentration sensitivity and (b) ranging precision.

The system reaches 0.6 ppm-m/√Hz sensitivity level with fiber coupled system. The free space experiment shows slightly worse performance due to signal loss with sensitivity of 3.0 and 1.7 ppm-m/√Hz without and with optical amplifier, respectively. Optical amplifier compensates for partially the signal loss, but introduces additional fringe that drifts at a faster rate (blue curve).

The ranging precision stays below the 0.1 m/√Hz goal for both fiber-coupled and free-space experiments, achieving 0.03 m/√Hz and 0.045 m/√Hz precision level respectively.

The heterodyne enhancement has been shown in Figure 1 in Task 3.1. Additional proof with diffusive targets are shown below in Figure 3, where enhancement as high as 23.9 dB is achieved.

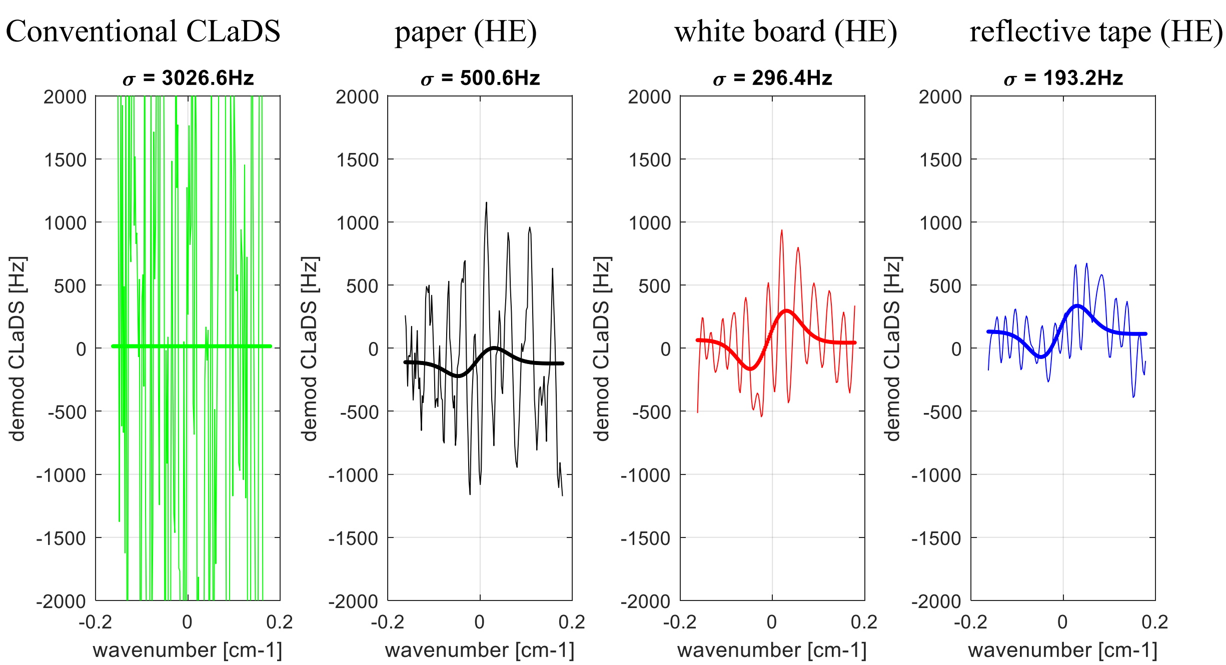

Figure 3. Signal enhancement and noise reduction with equivalent CNR enhancement (left to right) of 15.6 (paper as target), 20.2 (whiteboard), 23.9 dB (reflective tape).

Task 4: Outdoor testing and validation of system performance
Status: In progress

Research progress made:

- **Development of an outdoor calibration facility for 100 m roundtrip path and ability to provide controlled amounts of methane into the optical path**
- **Preliminary testing outside at the facility with the CLaDS system**

A calibration facility was developed for initial CLaDS remote sensing test in the outside environment. The facility consisted of a 50 m long duct pipe in a parking garage near the engineering laboratories. At one end was the CLaDS system containing the collection optics (telescope) and the far end housed a reflective surface. Ports along the tube allowed for controlled amounts of methane to be added to the pipe, and fans and flow controllers also allowed for regulated flows down the length of the tube. Figure 4 shows a schematic of the flow system that was tested in late June 2018. Figure 5 shows a photograph of the tube in the garage.

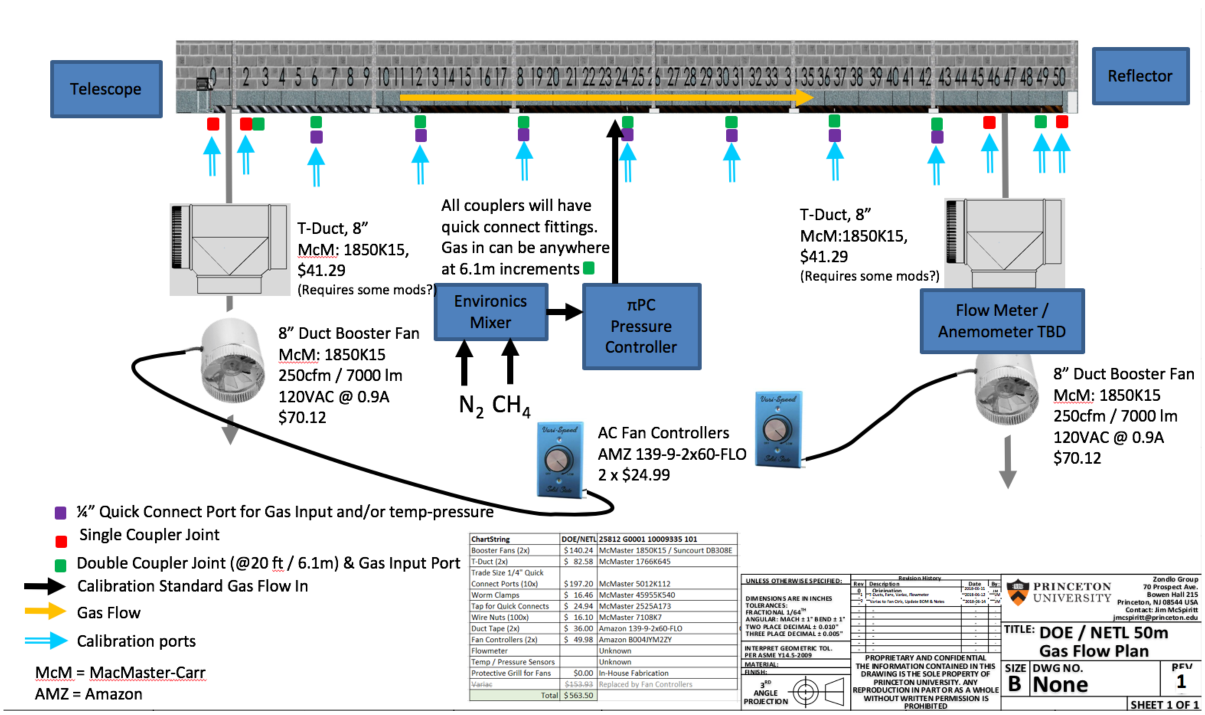

Figure 4. Schematic of the calibration facility for testing the HE-CLaDS system outside in a controlled manner. It consisted of a 50 m ducting tube with ports at selected distances for the introduction of calibrated, known amounts of methane. In addition, the flow down the tube could be adjusted for releasing methane standards at known distances downstream of the sensor. A LICOR LI-7700 open-path methane sensor was placed at the output of the 50 m tube to measure the concentrations inside the tube.

Figure 5. Photograph showing the CLaDS sensor (left) and the 50 m calibration tube (right) along the backside of a parking garage.

A long-term measurement was performed on outside air with ambient amounts of methane (2.0 ppmv). Ambient methane was measured by a LICOR 7700 open-path methane instrument at the sensor end of the calibration tube. The LICOR 7700 instrument was calibrated previously in the laboratory with a World Meteorological Organization/NOAA Global Monitoring Division standard of 1854 ± 3 ppbv in air, along with commercial gas standards at much higher concentrations in the 5-20 ppmv methane range (±5%, Air Liquide). The Allan plot for measurements of ambient methane is shown in Figure 6.

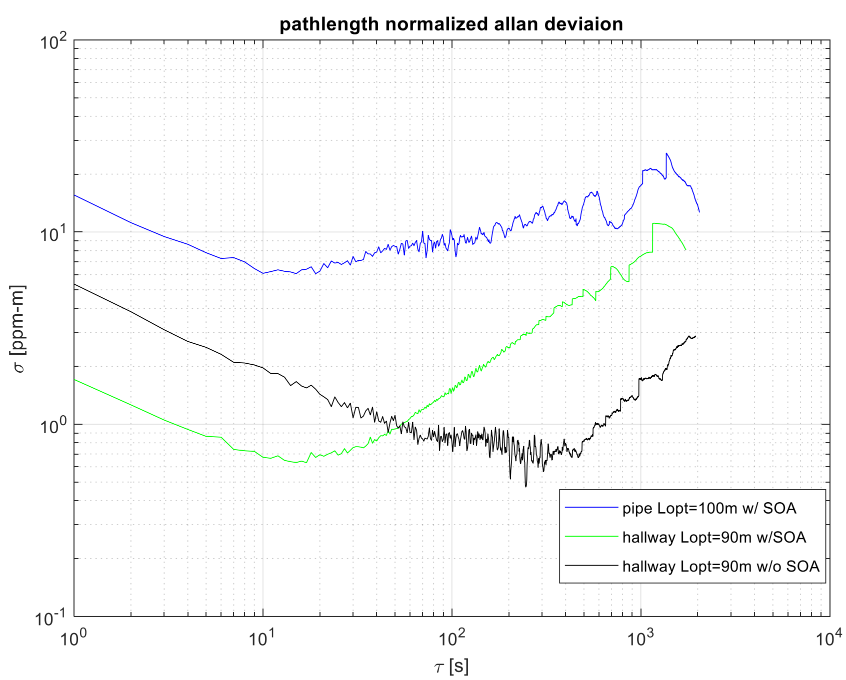

Figure 6. Sensitivity measurement in the 50 m long pipe in comparison with indoor characterization with and without the signal optical amplifier (SOA).

The bandwidth normalized sensitivity is one order of magnitude higher than those observed with indoor hallway tests. Two factors contribute to the result: (1) the laser beam is clipping inside the pipe which contributes to a much more severe signal loss compared with the open space during the hallway testing; and (2) the temperature fluctuation has a much higher range in the outdoor test and causes optics drifts (including fringes) in the system.

Nonetheless, even with the problems with these initial tests, the sensor was capable of seeing significant changes in methane at levels comparable to what is expected for pipeline leaks. Figure 7 shows an example where a 7 ppmv methane in air mixture was initially inside the tube. At t=700 s, the methane standard was turned off and instead the tube was flushed with ambient air (2 ppmv methane). A decrease is observed in the signal toward background conditions. The timescale (~ 300 s) in which this flushing took place is consistent with the flow rate down the pipe (~ 10 L s^{-1}) and pipe volume (3140 L).

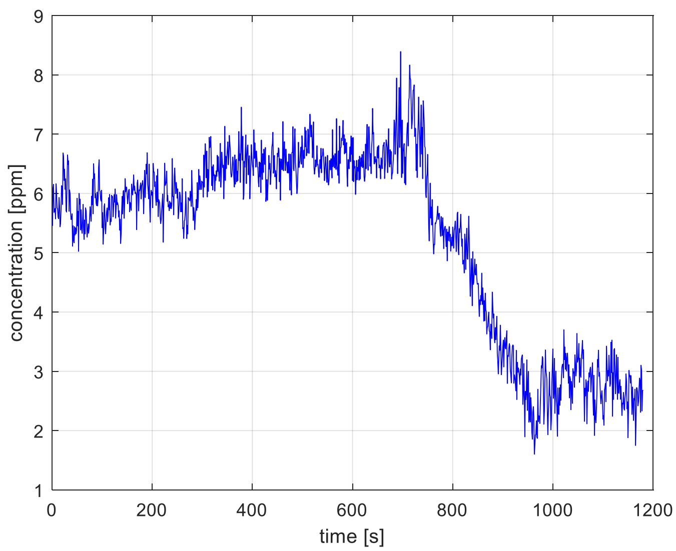

Figure 7. Timeseries of the CLaDS concentration inside the pipe while initially flowing a 7 ppmv methane standard. At t=700 s, the methane standard was turned off and ambient air at 2 ppmv was flushed into the calibration system. The signal decreases and approaches ambient conditions by the end of the timeseries.

Modifications to the setup are being conducted for the next quarter to minimize the signal clipping inside the tube and to improve the thermal stability of the optomechanical system.

Task 5: Development of tomographic reconstruction algorithms
Status: Not started yet, planned for August 2018

Task 6: Mobile field tests
Status: Not started yet, planned for October 2018

Task 7: Drone-based reflector target imaging
Status: Not started yet, planned for January 2019

Task 8: Airborne flight measurements
Status: Not started yet, planned for July 2019

Milestone Status Report

Milestone Title / Description	Planned completion	Actual completion	Verification method	Comments
A: Data management plan submitted	3/31/17	3/27/17	Accepted by program manager.	
B: System developed	2/28/18	2/28/18	Reported to program manager 3/22/18; appended to this report at end in Appendix A.	
C: Lab testing completed	8/31/18			
D: Field validation completed	10/31/18			
E: Tomographic algorithms	10/31/19			
F: Mobile field data collected	1/31/19			
G: Drone-based flights	9/30/19			
H: Manned aircraft flights	2/28/20			

Note: all dates extended by 5 month from the original proposal due to delays in paperwork at start but consistent with the relative timeframes in the SOPO with an effective start date of 3/1/17.

2c. Training and Professional Development
Not requested.

2d. Dissemination of Results / Outreach
No outreach events have occurred to communities of interest.

2e. Plans for Next Reporting Period
The calibration facility will be improved to remove beam clipping that we saw in the first tests, and additional tests will be conducted to finish the outdoor testing and calibrations.

3. Products
Publications, conference papers, and presentations
Publications
G. Plant, Y. Chen, and G. Wysocki, "Optical heterodyne-enhanced chirped laser dispersion spectroscopy," Optics Letters 42, 2770-2773 (2017).

Books or other non-periodical, one-time publications
None.

Other publications, conference proceedings, and presentations
Y. Chen, G. Plant, and G. Wysocki, "Heterodyne Efficiency in Chirped Laser Dispersion Spectroscopy," in Conference on Lasers and Electro-Optics(Optical Society of America, San Jose, California, 2017), p. SW4L.5.

Y. Chen, A. Hangauer, and G. Wysocki, "Path-averaged Methane Sensing Using Range-resolving Chirped Laser Dispersion Spectroscopy," in Laser Applications to Chemical, Security and Environmental Analysis (Optical Society of America, Florida, 2018), p. LTu5C-4.

4. Participants and other collaborators

American Aerospace Technologies Inc. (AATI), the commercial partner that will be flying the sensor on aircraft in Year 3 and who will fly a drone with a reflecting target in Year 2, has provided advice on aircraft constraints. These constraints play important roles in the overall design of the sensor while there is still time to adjust to any payload issues (or orientation). A conference call is occurring quarterly to identify any constraints in the system design for aircraft flights later in the project. The current design should integrate onto the Cessna 210 aircraft without a problem, according to David Yoel and Marty McGregor at AATI. The sensor was built to fit the aircraft constraints from the start of the project.

5. Impact (optional)

Nothing to report.

6. Changes and Problems

No changes or problems have been encountered. The project is on schedule and on specifications.

7. Special Reporting Requirements

No special reporting requirements (e.g. milestones) were scheduled to occur during this reporting period, and therefore no special reporting requirements are included.

8. Budgetary Information

Attached on the next page.

Baseline Reporting Quarter	Budget Period 1													
	Q1		Q2		Q3		Q4		Q5		Q6		Q7	
	10/1/2016-12/31/2016		1/1/2017-3/31/2017		4/1/2017-6/30/2017		7/1/2017-9/30/2017		10/1/17-12/31/17		1/1/18-3/31/18		4/1/18-6/30/18	
	Q1	Cumulative Total	Q2	Cumulative Total	Q3	Cumulative Total	Q4	Cumulative Total	Q5	Cumulative Total	Q6	Cumulative Total	Q7	Cumulative Total
Baseline Cost Plan														
Federal Share	78,189.71	78,189.71	78,189.71	156,379.42	78,189.71	234,569.13	78,189.71	312,758.84	78,189.71	390,948.55	78,189.71	469,138.26	78,189.74	547,328.00
Non-Federal Share	23,775.00	23,775.00	23,775.00	47,550.00	23,775.00	71,325.00	23,775.00	95,100.00	23,775.00	118,875.00	23,775.00	142,650.00	23,775.00	166,425.00
Total Planned	101,964.71	101,964.71	101,964.71	203,929.42	101,964.71	305,894.13	101,964.71	407,858.84	101,964.71	509,823.55	101,964.71	611,788.26	101,964.74	713,753.00
Actual Incurred Cost														
Federal Share	0.00	0.00	39,913.60	39,913.60	35,910.60	75,824.20	174,126.95	249,951.15	44,938.72	294,889.87	72,735.11	367,624.98	101,204.77	468,829.75
Non-Federal Share	0.00	0.00	2,361.00	2,361.00	38,538.35	40,899.35	34,510.39	75,409.74	19,632.34	95,042.08	34,049.88	129,091.96	36,310.08	165,402.04
Total Incurred Cost	0.00	0.00	42,274.60	42,274.60	74,448.95	116,723.55	208,637.34	325,360.89	64,571.06	389,931.95	106,784.99	496,716.94	137,514.85	634,231.79
Variance														
Federal Share	78,189.71	78,189.71	38,276.11	116,465.82	42,279.11	158,744.93	(95,937.24)	62,807.69	33,250.99	96,058.68	5,454.60	101,513.28	(23,015.03)	78,498.25
Non-Federal Share	23,775.00	23,775.00	21,414.00	45,189.00	(14,763.35)	30,425.65	(10,735.39)	19,690.26	4,142.66	23,832.92	(10,274.88)	13,558.04	(12,535.08)	1,022.96
Total Variance	101,964.71	101,964.71	59,690.11	161,654.82	27,515.76	189,170.58	(106,672.63)	82,497.95	37,393.65	119,891.60	(4,820.28)	115,071.32	(35,550.11)	79,521.21